Nonlinear dynamics of the TMMC chain

1996 J. Phys.: Condens. Matter 8 5437

(http://iopscience.iop.org/0953-8984/8/29/017)

J. Phys.: Condens. Matter **8** (1996) 5437–5450. Printed in the UK

Nonlinear dynamics of the TMMC chain

Rodrigo Ferrer†

Departamento de Física, Facultad de Ciencias, Universidad de Chile, Casilla 653, Santiago, Chile

Received 19 December 1995, in final form 26 April 1996

Abstract. We investigate the integrability of the TMMC antiferromagnetic chain in a transverse external magnetic field for the x–y and y–z planar configurations. It is shown that the system is nonintegrable even when the magnetic external field and the anisotropy are not present simultaneously.

The problem investigated in this paper is that of the nature of some low-temperature nonlinear magnetic excitations in the easy-plane spin-5/2 anisotropic antiferromagnetic chain $(CH_3)_4$–$NMnCl_3$ (TMMC). Nuclear spin–lattice relaxation measurements [1] in the presence of an external magnetic field, perpendicular to the chain direction, have been performed on different nuclei of this magnetic chain, showing an interesting behaviour of T_1^{-1}: it increases exponentially as a function of the external field, at fixed temperature. A simple sine–Gordon theory explains these results for fields under 40 kOe; there T_1^{-1} decreases with the field. For stronger fields the increase of T_1^{-1} suggests a deviation from the sine–Gordon theory since it may be interpreted by a switching of the roles of the magnetic field and the anisotropy [2]. Consequently, two extreme cases are predicted to occur as regards low-temperature excitations: first, a soliton consisting in a rotation of the spins up to an angle π from an antiferromagnetic or a spin-flop order in a plane perpendicular to the chain direction (x–y soliton), and second, an analogous rotation but now in a plane containing the chain direction (y–z soliton). The chain direction is taken to be the z-axis.

Literature pertinent to magnetic excitations in this system can be found in [2–9].

We are interested in the analysis of the coherent and chaotic structures of the TMMC chain. A complete analysis of these structures has been performed in [10] for a classical continuum anisotropic ferromagnetic chain in the presence of a transverse field; it is found that this chain is integrable only in the absence of either the anisotropic interaction or the external magnetic field. For nonintegrability, it is important to consider [11] for a classical nonintegrable triangular three-spin system with antiferromagnetic exchange coupling.

The formalism used in this paper is that of the coherent states applied to a Heisenberg Hamiltonian. Spin operators are transformed in operators of two independent harmonic oscillators using Schwinger transformations [12]. Making use of the semi-classical approximation in which the spins are considered as continuously projected along the quantization axis we write down the equations of motion for these operators and project in the basis of coherent states, obtaining nonlinear difference equations for variables that are easy to interpret in terms of physical magnitudes. For simplicity we consider only the extreme cases: x–y and y–z solitons; nevertheless the theory is for the general case where

† E-mail: rferrer@macul.ciencias.uchile.cl.

0953-8984/96/295437+14$19.50

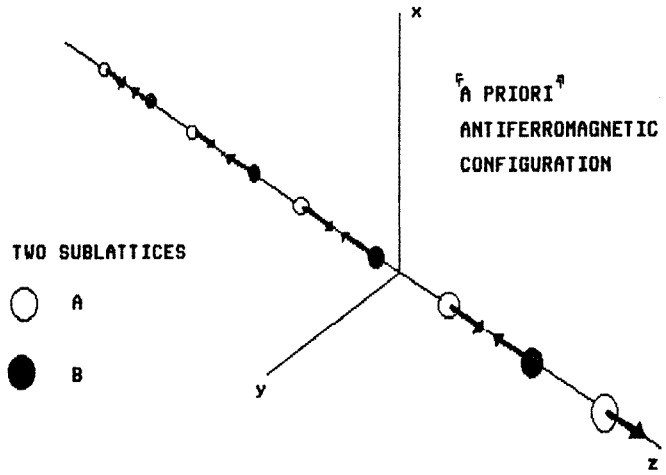

Figure 1. Antiferromagnetic ordering of the two sublattices on the basis of which the system is described using Hamiltonian (2).

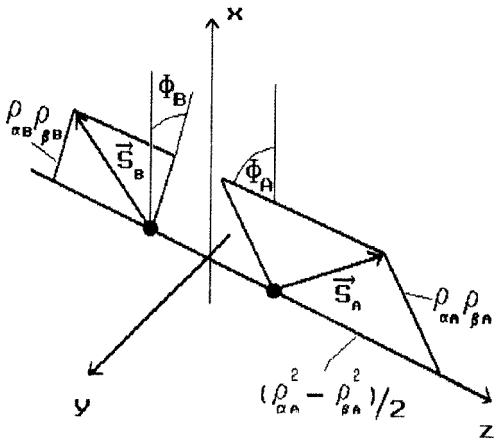

Figure 2. The geometry affecting two neighbouring spins in the antiferromagnetic chain.

both kinds of excitation are present, i.e., when the external field and the anisotropy are present simultaneously. The extreme cases correspond to static configurations that may also be obtained by minimizing the energy of the general coherent state.

Our study considers the chain modelled by an easy-plane Heisenberg Hamiltonian:

$$H = \frac{J}{2}\sum_{n=1}^{N}\sum_{\delta=\pm1} \boldsymbol{S}_n \cdot \boldsymbol{S}_{n+\delta} + D\sum_{n=1}^{N}(S_n^z)^2 - h\sum S_n^x \tag{1}$$

where $J > 0$ is the antiferromagnetic nearest-neighbour exchange interaction, $D > 0$ is the anisotropy parameter and $h \equiv g\mu_B H$ with H the intensity of the external magnetic field in the x-direction perpendicular to the chain. g is the g-factor and μ_B is the Bohr magneton. The label n represents the lattice sites.

As we will not work with small deviations of the spins with respect to any axis, we

describe the deviations from an *a priori* antiferromagnetic state in a two- (A and B) sublattice model, as indicated in figure 1. Then, there exists the following correspondence between the raising and the lowering spin operators acting on each sublattice:

$$S_A^\dagger \leftrightarrow S_B^- \qquad S_A^- \leftrightarrow S_B^\dagger \qquad S_A^z \leftrightarrow -S_B^z. \tag{2}$$

In this way, $S_A^x \leftrightarrow S_B^x$ and $S_A^y \leftrightarrow -S_B^y$.

In terms of these operators the Hamiltonian takes the form

$$H = \frac{J}{2}\sum_{n=1}^{N}\sum_{\delta=\pm1}\left[\frac{1}{2}(S_n^\dagger S_{n+\delta}^\dagger + S_n^- S_{n+\delta}^-) - S_n^z S_{n+\delta}^z\right] + D\sum_{n=1}^{N}(S_n^z)^2 - \frac{h}{2}\sum_{n=1}^{N}(S_n^\dagger + S_n^-). \tag{3}$$

To complete the picture we make use of the Schwinger transformations linking the spin operators with two independent bosonic fields:

$$S^z = \frac{1}{2}(a^\dagger a - b^\dagger b) \qquad S^\dagger = a^\dagger b \qquad S^- = b^\dagger a \tag{4}$$

where a and b are the lowering operators of two simple harmonic oscillators with the constraint $a^\dagger a + b^\dagger b = 2S$ on the total Bose occupation. In this representation the Hamiltonian can be treated in the framework of the coherent states [13], in which we define the displacement operators

$$D(\alpha_n) = \exp(\alpha_n a_n^\dagger - \alpha_n^* a_n) \tag{5}$$

$$D(\beta_n) = \exp(\beta_n b_n^\dagger - \beta_n^* b_n) \tag{6}$$

where α_n and β_n are complex numbers. Taking a semi-classical approach for the projections of the spins and denoting by $|\mathrm{AF}\rangle$ the configuration of figure 1, the excited states are

$$|\alpha_n\beta_n\rangle = |\alpha_n\rangle|\beta_n\rangle = D(\alpha_n)D(\beta_n)|\mathrm{AF}\rangle \tag{7}$$

and the coherent states $|\alpha_n\rangle$ and $|\beta_n\rangle$ have the forms

$$|\alpha_n\rangle = \exp\left(-\frac{1}{2}\alpha_n^*\alpha_n\right)\sum_{\nu=0}^{\infty}\frac{\alpha_n^\nu}{\sqrt{\nu!}}|\nu\rangle \tag{8}$$

$$|\beta_n\rangle = \exp\left(-\frac{1}{2}\beta_n^*\beta_n\right)\sum_{\nu=0}^{\infty}\frac{\beta_n^\nu}{\sqrt{\nu!}}|\nu\rangle \tag{9}$$

which are eigenstates of the annihilation operators a_n and b_n with eigenvalues α_n and β_n, respectively, and $|\nu\rangle$ is the eigenstate of the simple harmonic oscillator.

The general coherent state of the system is

$$|\alpha\beta\rangle = \prod_n |\alpha_n\beta_n\rangle \tag{10}$$

giving for the average energy in that state

$$\begin{aligned}\langle H\rangle = \langle\alpha\beta|H||\alpha\beta\rangle = \frac{J}{2}\sum_{n,\delta\pm1}\Bigg[&\frac{1}{2}(\beta_n\beta_{n+\delta}\alpha_n^*\alpha_{n+\delta}^* + \alpha_n\alpha_{n+\delta}\beta_n^*\beta_{n+\delta}^*)\\ &- \frac{1}{4}(|\alpha_n|^2 - |\beta_n|^2)(|\alpha_{n+\delta}|^2 - |\beta_{n+\delta}|^2)\Bigg]\\ &+ \frac{D}{4}\sum_n(|\alpha_n|^2) - |\beta_n|^2)^2 - \frac{h}{2}\sum_n(\alpha_n^*\beta_n + \beta_n^*\alpha_n).\end{aligned} \tag{11}$$

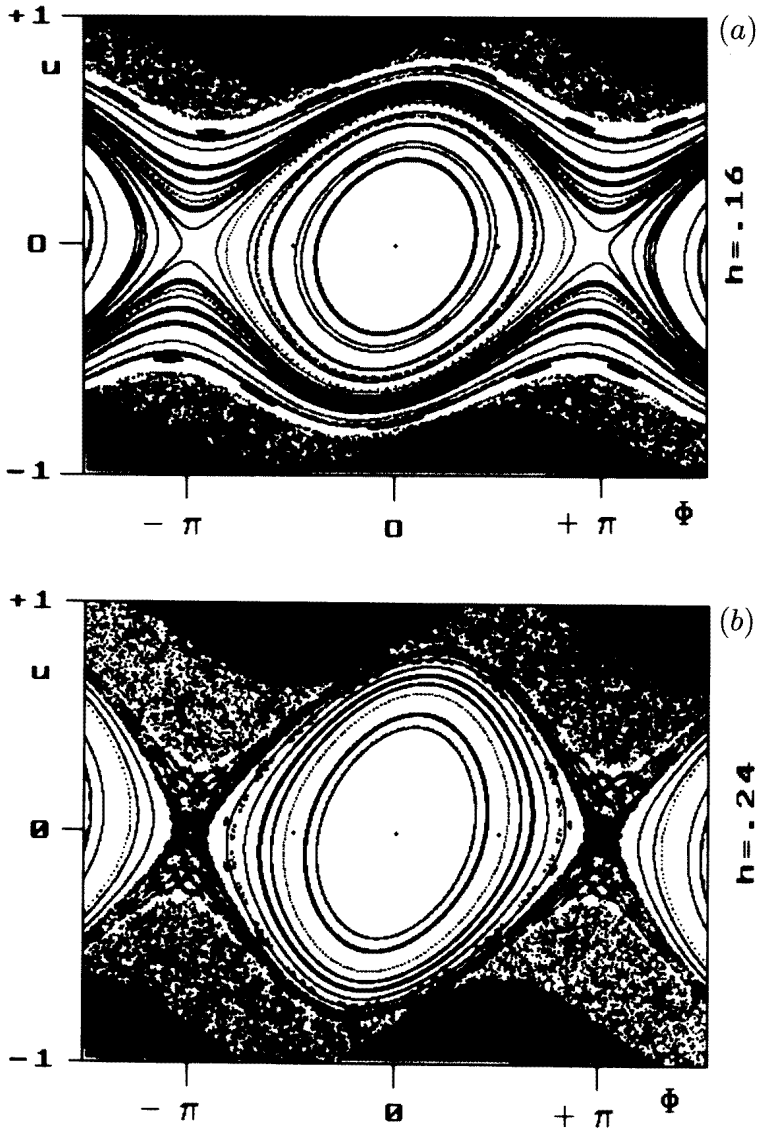

Figure 3. Poincaré mappings in the Φ–u space for the x–y equilibrium configuration of the spins for two values of the external magnetic field h: (*a*) $h = 0.16$; (*b*) $h = 0.24$.

Writing the complex numbers α_n and β_n in the polar representation, $\alpha_n = \rho_{\alpha n}\exp(\mathrm{i}\phi_{\alpha n})$ and $\beta_n = \rho_{\beta n}\exp(\mathrm{i}\phi_{\beta n})$, this average takes the form

$$\langle H\rangle = \frac{J}{2}\sum_n [\rho_{\alpha n}\rho_{\alpha n+1}\rho_{\beta n}\rho_{\beta n+1}\cos(\Phi_{n+1}+\Phi_n) + \rho_{\alpha n}\rho_{\alpha n-1}\rho_{\beta n}\rho_{\beta n-1}\cos(\Phi_{n-1}+\Phi_n)]$$
$$- \frac{J}{8}\sum_n (\rho_{\alpha n}^2 - \rho_{\beta n}^2)[(\rho_{\alpha n+1}^2 - \rho_{\beta n+1}^2) + (\rho_{\alpha n-1}^2 - \rho_{\beta n-1}^2)]$$
$$+ \frac{D}{4}\sum_n (\rho_{\alpha n}^2 - \rho_{\beta n}^2)^2 - h\sum_n \rho_{\alpha n}\rho_{\beta n}\cos\Phi_n \qquad (12)$$

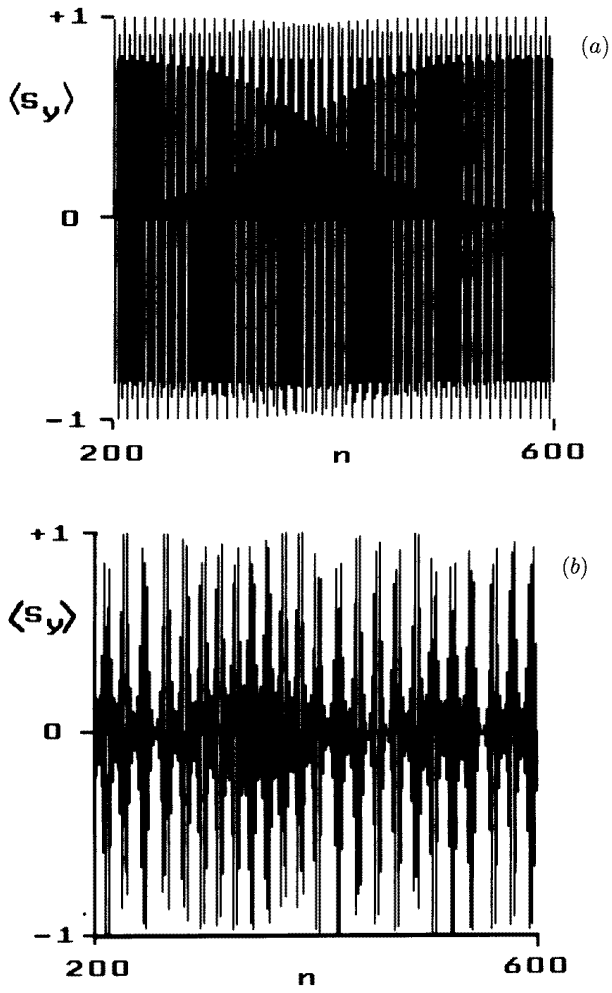

Figure 4. For the x–y excitations, (a) $\langle S_y \rangle$ on each site for ($\Phi_{initial} = 0.7$, $u_{initial} = 0.01$) and $h = 0.228\,786\,6666$, (b) $\langle S_y \rangle$ on each site for ($\Phi_{initial} = 0.98$, $u_{initial} = 0.01$) and $h = 0.239\,9994$.

where $\Phi_n \equiv \phi_{\alpha n} - \phi_{\beta n}$; the physical meaning of Φ_n is obtained when we take the averages of the spin operators S_n^x, S_n^y and S_n^z in this state:

$$\begin{aligned} \langle S_n^x \rangle &= \rho_{\alpha n}\rho_{\beta n} \cos \Phi_n \\ \langle S_n^y \rangle &= \pm \rho_{\alpha n}\rho_{\beta n} \sin \Phi_n \\ \langle S_n^z \rangle &= \pm \frac{1}{2}(\rho_{\alpha n}^2 - \rho_{\beta n}^2). \end{aligned} \tag{13}$$

Here $\pm$ stands for the A ($+$) and B ($-$) sublattices. In figure 2 we make clear the geometry affecting two neighbouring spins.

The equations of motion are obtained from the Heisenberg equations $i\dot{a}_n = [a_n, H]$ and

$i\dot{b}_n = [b_n, H]$; we find

$$
\begin{aligned}
i\dot{a}_n &= \frac{J}{2}a^{\dagger}_{n+1}b_{n+1}b_n + \frac{J}{2}a^{\dagger}_{n-1}b_{n-1}b_n + Ja_n[n^a_{n+1} - n^b_{n+1} + n^a_{n-1} - n^b_{n-1}] \\
&\quad + D(1 + 2(n^a_n - n^b_n))a_n - \frac{h}{2}b_n \\
i\dot{b}_n &= \frac{J}{2}b^{\dagger}_{n+1}a_{n+1}a_n + \frac{J}{2}b^{\dagger}_{n-1}a_{n-1}a_n + Jb_n[n^b_{n+1} - n^a_{n+1} + n^b_{n-1} - n^a_{n-1}] \\
&\quad + D(1 + 2(n^b_n - n^a_n))b_n - \frac{h}{2}a_n
\end{aligned}
\tag{14}
$$

with $n^a_n \equiv a^{\dagger}_n a_n$ and $n^b_n \equiv b^{\dagger}_n b_n$.

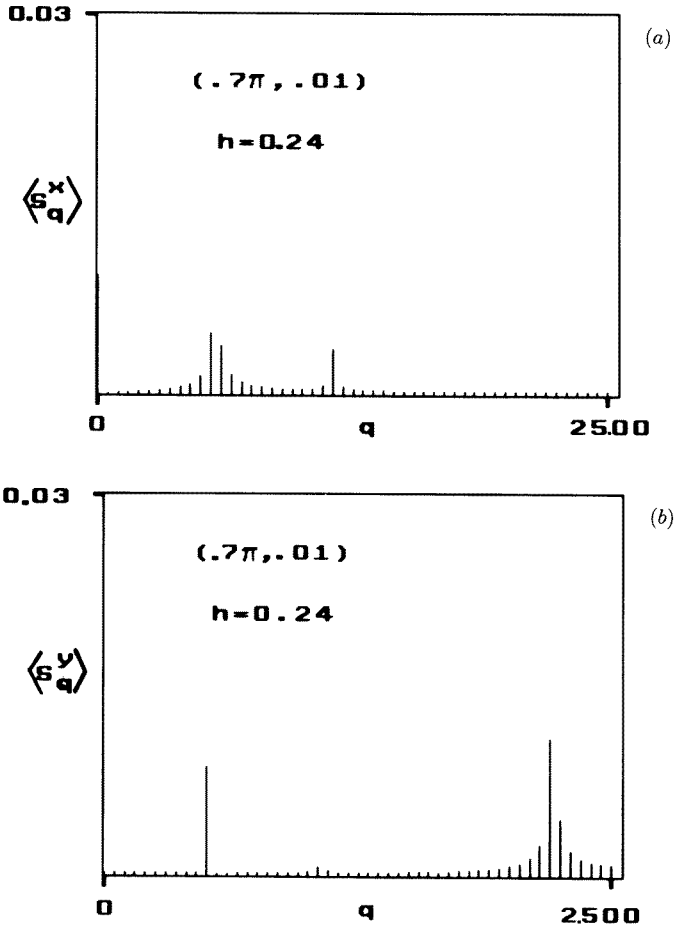

Figure 5. For the x–y excitations, absolute values of the Fourier transforms (*a*) $\langle S^x_q \rangle$ and (*b*) $\langle S^y_q \rangle$; the quantities in parentheses represent the initial values of Φ and u.

When these equations are projected into the coherent space we obtain the equations of motion for α_n and β_n, i.e., for $\rho_{\alpha n}$, $\rho_{\beta n}$ and Φ_n, which with (13) give the dynamics of the averaged spin operators.

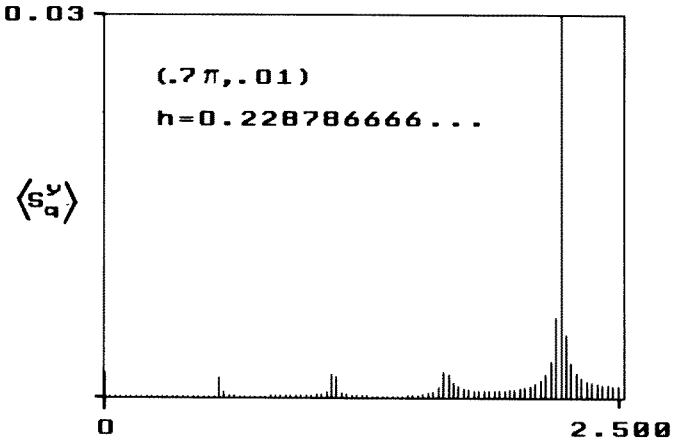

Figure 6. For the x–y excitations, absolute values of the Fourier transforms $\langle S_q^y \rangle$; the quantities in parentheses represent the initial values of Φ and u.

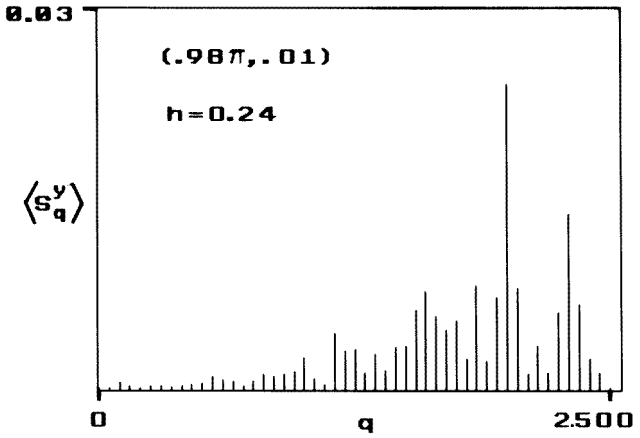

Figure 7. For the x–y excitations, chaotic structure of the absolute value of the Fourier transform $\langle S_q^y \rangle$; the quantities in parentheses represent the initial values of Φ and u.

We consider now the two extreme cases: x–y and y–z solitons.

For the x–y soliton we take the condition $\langle S_n^z \rangle \equiv 0$ at each site, which means $\langle n_n^a - n_n^b \rangle = 0$ for all n. In this case we obtain the equation

$$-\mathrm{i}\dot{\Phi}_n = \sin(\Phi_{n+1} + \Phi_n) + \sin(\Phi_{n-1} + \Phi_n) - h \sin \Phi_n. \tag{15}$$

As expected this discrete nonlinear difference equation is independent of the anisotropy and corresponds to a static configuration, since it gives $\dot{\Phi}_n = 0$. In fact we can deduce equation (15) by minimizing $\langle H \rangle$ with respect to the coherent-state parameters Φ_n and $\rho_{\alpha n}$ ($\partial \langle H \rangle / \partial \Phi_n = 0$, $\partial \langle H \rangle / \partial \rho_{\alpha n} = 0$) with the Schwinger constraint now in the form $\rho_{\alpha n}^2 + \rho_{\beta n}^2 = 2S$. This static configuration is a well known attribute of the planar solitons. We must keep in mind that relation (15) holds for both sublattices and that the difference between the lattices is given in equations (13).

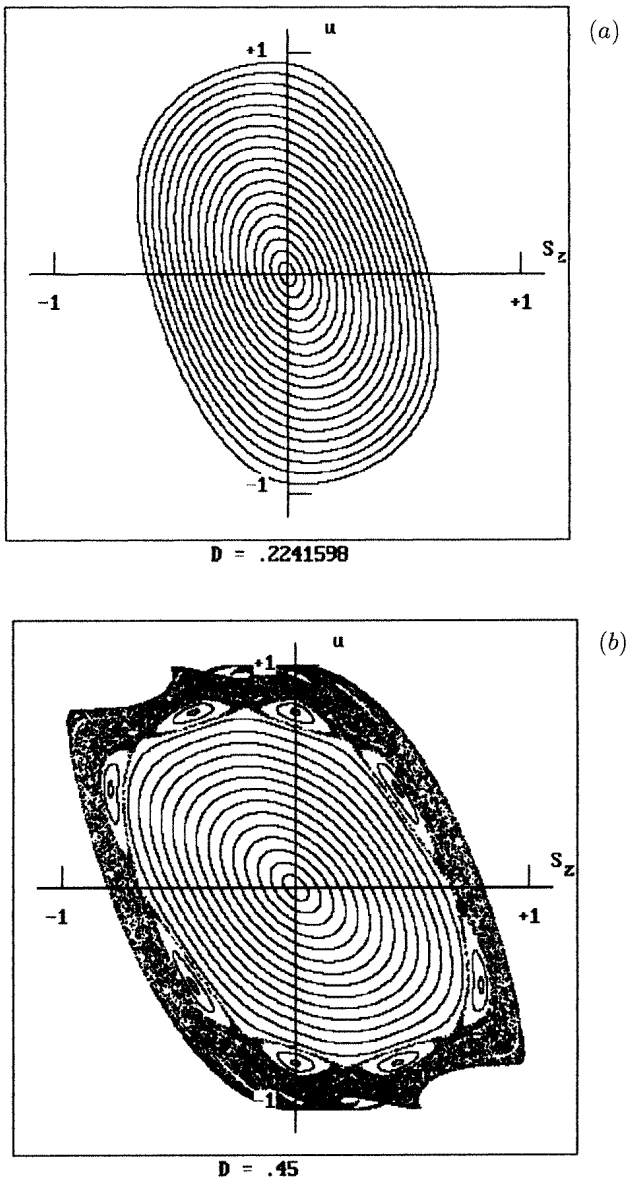

Figure 8. Poincaré mappings of the y–z excitations in the u–S^z phase space. (a) $D = 0.224\,1598$; (b) $D = 0.45$; (c) $D = 0.63$ (note the zoom).

Defining $u_{n+1} \equiv \sin(\Phi_{n+1} + \Phi_n)$, we construct from (15) the maps

$$\begin{aligned} \bar{u} &= -u + h \sin \Phi \\ \bar{\Phi} &= -\Phi + \nu\pi + (-1)^{\nu} \arcsin \bar{u} \end{aligned} \tag{16}$$

where $\nu = 0$ or 1, $\bar{u} \equiv u_{n+1}$, $u \equiv u_n$, $\bar{\Phi} \equiv \Phi_{n+1}$ and $\Phi \equiv \Phi_n$.

We first note that in the phase space Φ–u this map has a fixed point at ($\Phi = \arccos(h/4), u = 0$), which corresponds to the well known spin-flop configuration; this

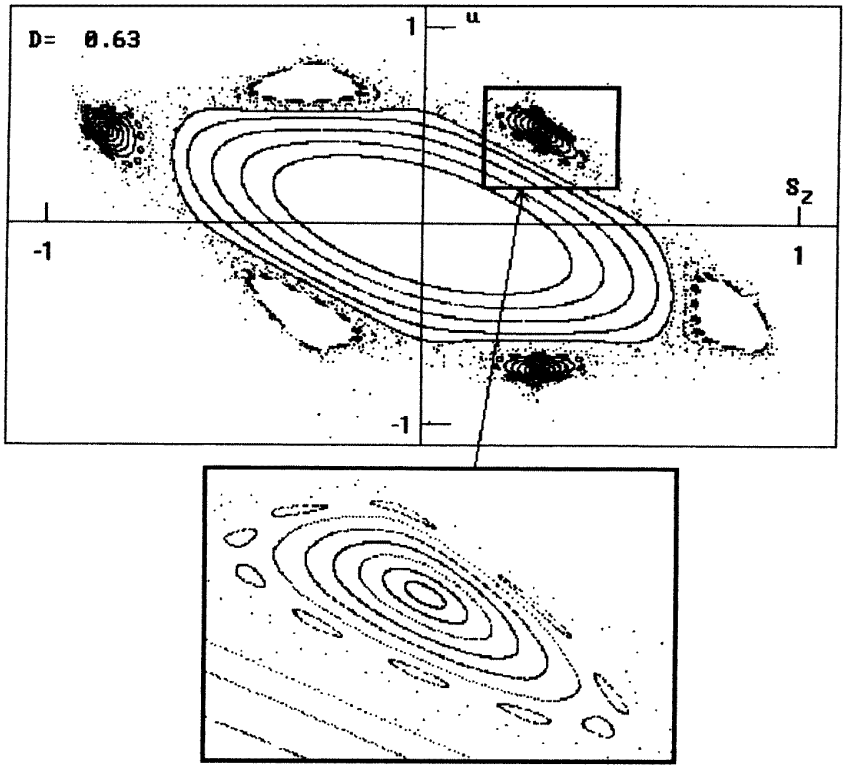

(*c*)

Figure 8. (Continued)

is a stable point in the phase space. However, not all of the points in the phase space correspond to stable situations. Sinai's stochasticity criterion imposes the diagonalization of the matrix:

$$M = \begin{pmatrix} \partial\bar{\Phi}/\partial\Phi & \partial\bar{\Phi}/\partial u \\ \partial\bar{u}/\partial\Phi & \partial\bar{u}/\partial u \end{pmatrix}. \tag{17}$$

As $\det M = 1$ the maps (16) preserve the area. The characteristic values are

$$\lambda_{1,2} = -1 + 0.5K_1K_2\left(1 \pm \sqrt{1 - \frac{4}{K_1K_2}}\right) \tag{18}$$

where

$$K_1 \equiv h\Phi \qquad K_2 \equiv 1/\sqrt{1 - (h\sin\Phi - u)^2}. \tag{19}$$

To illustrate the regions of stability, i.e., where $|\lambda_{1,2}| < 1$, we scan the Φ–u plane, for different values of the magnetic field. Deep-shaded areas in figure 3 correspond to points with $|\lambda_{1,2}| > 1$ (instability), and the sparsely dotted areas are for initial values giving a nonconsistent mapping; in fact, there we have forced periodicity in the u-variable. For small values of h all of the initial values of u and Φ give stable motion, in agreement with the Kolmogorov–Arnold–Moser (KAM) theorem, and we see the presence of separatrixes with hyperbolic points at points $(\Phi = n\pi, u = 0)$.

Increasing the field h causes local instabilities, resulting in a mixing of trajectories in the phase space for some initial points in the neighbourhood of the separatrixes. Also the existence of stability islands as h increases is confirmed in these patterns—this is a fundamental property of real physical systems; the number of stability islands increases with h and we see a variety of sizes and shapes. Smooth regular regions are abundant, and within these regions there are chaotic regions; the system is then nonintegrable and satisfies the KAM theorem. Note also that the stochasticity for a given value of h is strongly dependent on the relative initial positions of the spins on each sublattice; for example, if $h = 0.24$ and $\Phi_{initial} = 0.7\pi$, the motion is regular if $u_{initial} = 0$ and stochastic if $u_{initial} = 0.3$. In all of our calculations we take $J = 1$. The route to chaos in these x–y excitations seems to be the intermittency; figure 4(a) shows $\langle S^y \rangle$ on each site for initial conditions $(0.7\pi, u = 0.01)$ and $h = 0.228\,786\,6666$, making clear the existence of different frequencies and the presence of x–y solitons, i.e., the flip of the spins. The case of chaotic structure for $\langle S^y \rangle$ is seen in figure 4(b) where $h = 0.239\,9994$ and for the initial conditions $(0.98\pi, 0.01)$.

The equivalent dynamic system is obtained after finding a Hamiltonian leading to the equations of motion whose solutions are the maps in (16). For our system the equivalent Hamiltonian is:

$$H_e = \nu\pi u + (-1)^\nu \left[u \arcsin u + \sqrt{1-u^2} \right] + \left[2h \cos^2 \frac{\Phi}{2} + 2u\Phi \right] \sum_{j=0}^{N} \delta(x-j) \tag{20}$$

where the j are the positions of the lattice and the x-coordinate plays the role of time. The Hamilton equations are

$$\frac{\mathrm{d}u}{\mathrm{d}x} = -\frac{\partial H}{\partial \Phi} = [h \sin \Phi - 2u] \sum_{j=0}^{N} \delta(x-j) \tag{21}$$

$$\frac{\mathrm{d}\Phi}{\mathrm{d}x} = \frac{\partial H}{\partial u} = \nu\pi + (-1)^\nu \arcsin u + 2\Phi \sum_{j=0}^{N} \delta(x-j). \tag{22}$$

Between the lattice points $\mathrm{d}u/\mathrm{d}x = 0$ and we have a free rotation with frequency $\nu\pi + (-1)^\nu \arcsin u$ $(\nu = 0, 1)$. The equivalent dynamic system is then a nonlinear pendulum with that frequency and perturbed by kicks with unit period. Finally, the map is obtained by integrating in the neighbourhood of the δ-function.

The structure of the chain of spins is given by the averages $\langle S^x \rangle$ and $\langle S^y \rangle$. A question immediately arises as to whether there exists some kind of short-range order. To answer this we find it convenient to describe their spectral properties in terms of the corresponding Fourier transforms:

$$\begin{aligned} \langle S^x_q \rangle &= \frac{1}{N} \sum_{n=0}^{N-1} \cos \Phi_n \exp(-\mathrm{i}\, 2\pi n q/N) \\ \langle S^y_q \rangle &= \frac{1}{N} \sum_{n=0}^{N-1} \sin \Phi_n \exp(-\mathrm{i}\, 2\pi n q/N). \end{aligned} \tag{23}$$

In figure 5 we show $|\langle S^x_q \rangle|$ and $|\langle S^y_q \rangle|$ as functions of discrete values of q for $h = 0.24$ and the initial condition $(\Phi = 0.7\pi, u = 0.01)$. We observe relatively large amplitudes at $q = 500 \approx N/10$ and $q = 2200 \approx N/2$ for the y-component, indicating an anti-ferromagnetic order with one subharmonic. For the x-component the maxima are at $q = 0$, $q = 550$ and $q = 1100$ indicating a ferromagnetic order with two subharmonics. For $h = 0.228\,787$ and the above initial conditions we obtained the pattern of figure 6,

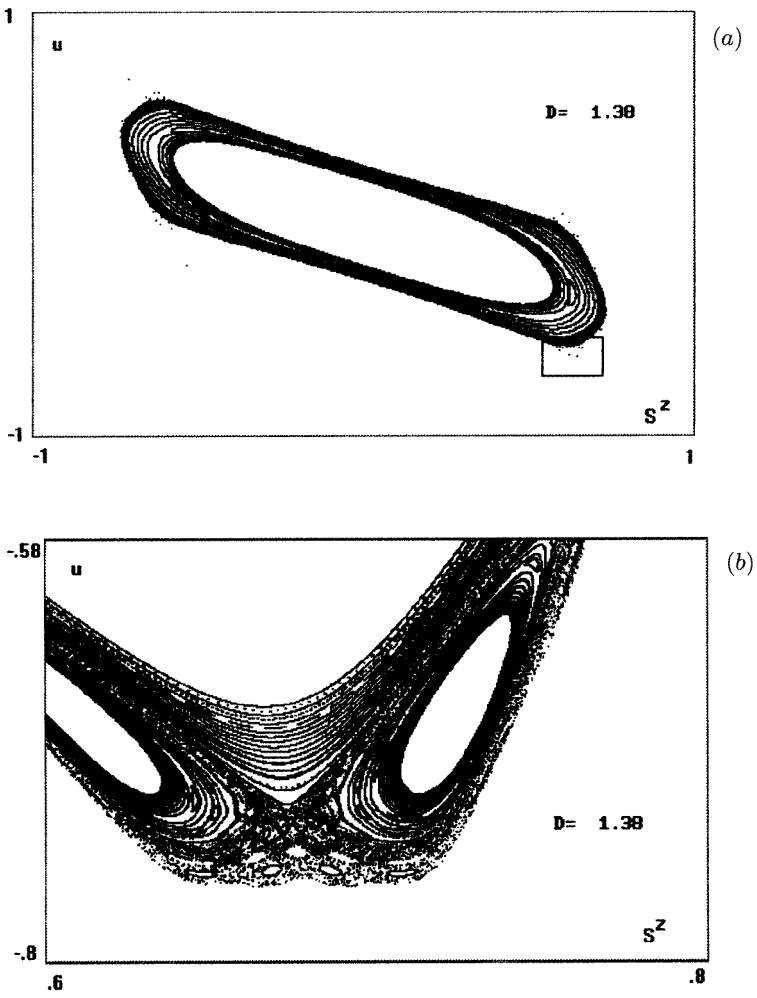

Figure 9. Poincaré mappings of the y–z excitations in the u–S^z phase space for $D = 1.38$. (a) The whole region, and (b) the region of the rectangle in (a).

demonstrating a case of antiferromagnetic order of the y-component. The chaotic structure is seen in figure 7 for $h = 0.24$ and initial conditions $(0.98\pi, 0.01)$; the stochastic amplitudes are larger near $N/2$, demonstrating the existence of short antiferromagnetic order.

We turn now to the case of the y–z solitons. In this case the condition for the solutions of equations (14) is $\Phi_j = \pi/2$ for all j. The time-independent, h-independent equations describing the ground state of the spins are

$$S^y_{j+1}S^z_j + S^y_{j-1}S^z_j - S^y_j S^z_{j+1} - S^y_j S^z_{j-1} + 2D\, S^y_j S^z_j = 0. \tag{24}$$

This difference equation is obtained together with equation (15) when we minimize $\langle H \rangle$ in the form already described.

The consistent mapping for these excitations is constructed by defining $u_{j+1} \equiv S^y_{j+1}S^z_j -$

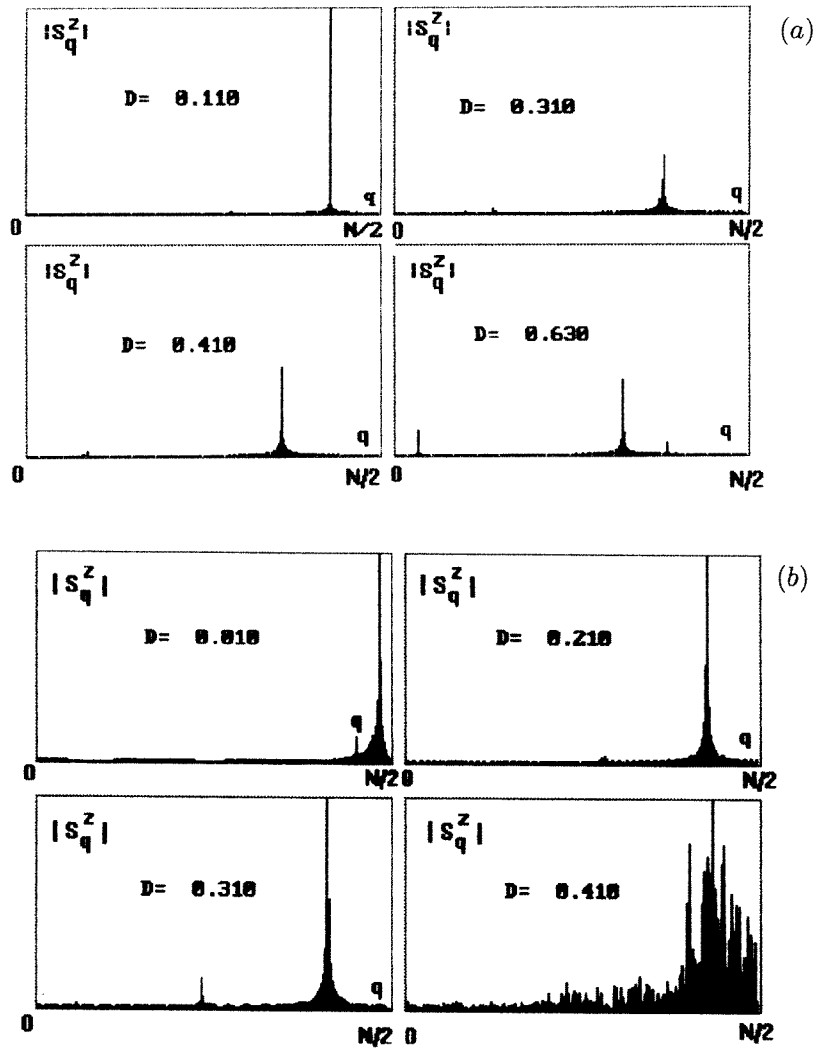

Figure 10. For the y–z excitations, the absolute value of the Fourier transform S^z_q for different values of the anisotropy, (a) for the initial conditions ($S^z = 0.49$, $u = 0$), and (b) for the initial conditions ($S^z = 0.887$, $u = 0$).

$S^y_j S^z_{j+1}$; we obtain

$$\begin{aligned} \bar{u} &= -u - 2D\sqrt{1-(S^z)^2}S^z \\ \bar{S}^z &= -\bar{u}\sqrt{1-(S^z)^2} - \sqrt{1-\bar{u}^2}S^z. \end{aligned} \tag{25}$$

As the spins have $S^x_j = 0$ for all j, u_{j+1} is simply equal to $|\boldsymbol{S}_{j+1} \times \boldsymbol{S}_j|$ and we have a simple physical interpretation for u. A fixed point of the map (25) is the point ($S^z = 0, u = 0$). However, for $D = 2$ we obtain a curve of fixed points: $u = -2\sqrt{1-(S^z)^2}S^z$ when $|S^z| \leqslant \sqrt{2}/2$.

Iterations corresponding to (25) are presented in figure 8 for three values of the

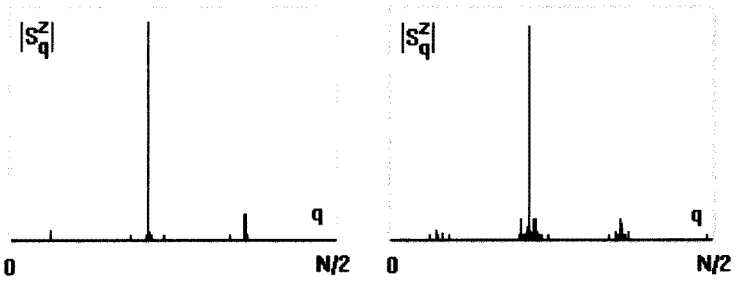

Figure 11. For the y–z excitations, regular behaviour of the absolute value of the Fourier transform S_q^z for $D = 1.38$ and for the initial conditions ($S^z = 0.6231$, $u = -0.63512$) (left-hand panel); and chaotic behaviour of this magnitude for the initial conditions ($S^z = 0.6105$, $u = -0.635\,12$) (right-hand panel).

anisotropy D. It is seen that regularity tends to disappear with D, existing chaotic zones and an abundance of regular regions between them (KAM). After an interesting orbit of period four obtained for $D = 1$, i.e., when the anisotropy equals the antiferromagnetic interaction J, we get for $D > 1$ regular orbits and stochastic orbits depending on the initial conditions; see figure 9. As before, D favours stochasticity, and again there are regular regions inserted in the stochastic sea.

Let us consider the corresponding spectral analysis for these excitations. We define

$$S_q^z = \frac{1}{N}\sum_{n=0}^{N-1} S_n^z \exp(-\mathrm{i}\,2\pi nq/N). \tag{26}$$

In this way the eight islands in figure 9 are characterized with $q = 256$. There $D = 0.45$ and the eight points correspond to an orbit with $S^z_{initial} = 0.72$ and $u_{initial} = 0$; in fact $|S_q^z|$ is peaked at $q = 256 = 2048/8$ for a chain with $2^{11} = 2048$ spins. Obviously, the case where $D = 1$ gives a peak at $q = 512$.

Let $D < 1$ and consider the two cases corresponding to the initial conditions ($S^z_{initial} = 0.49$, $u_{initial} = 0$) and ($S^z_{initial} = 0.887$, $u_{initial} = 0$). In the first case the KAM torus is never destroyed for $0 < D < 1$ and the spectrum shows that $|S_q^z|$ has its first peak near $q = N/2$ for small D, and the peak then moves towards smaller values of q, and that there are subharmonics, one of them near $q = 0$, indicating that D does not favour the antiferromagnetic short-range correlations; see figure 10(a). The second case is the one where the KAM torus can be destroyed for large enough D. The spectrum is shown in figure 10(b) where short-range order antiferromagnetism is always present.

For the case where $D > 1$ the KAM torus is destroyed for some values of the anisotropy and initial conditions—for example, taking $D = 1.38$ and the initial conditions ($S^z_{initial} = 0.6105$, $u_{initial} = -0.635\,12$); see figure 9. For the same D and the initial conditions ($S^z_{initial} = 0.6231$, $u_{initial} = -0.635\,12$) the orbit is regular. In figure 11 we present the spectrum corresponding to these two cases. Both cases present three peaks near the same values of q, but the stochastic case has broader peaks: a route to chaos.

Summarizing, we have investigated the excitations of the antiferromagnetic chain in two extreme cases: x–y solitons and y–z solitons. In the first case only the magnetic field is present while in the second only anisotropy is present. In both cases we have static spatial configurations. As regards the integrability, the system is nonintegrable even in the

absence of anisotropy or an external field—in contrast with the case of a ferromagnetic chain with uniaxial anisotropy [10]. A Fourier analysis allows us to determine the existence of periodic orbits and the existence of fundamentals and harmonic periods of the spatial structure. Finally, it seems that it may be useful to investigate the case where both the external field and anisotropy are simultaneously present; the equations that must be solved are given in (14) and deserve future investigation.

References

[1] Boucher J P and Renard J P 1980 *Phys. Rev. Lett.* **45** 486
[2] Benner H, Seitz H, Wiese J and Boucher J P 1984 *J. Magn. Magn. Mater.* **45** 354
[3] Harada I, Sasaki H and Shiba D 1981 *Solid State Commun.* **40** 29; 1984 *Solid State Commun.* **45** 354
[4] Fluggen N and Mikeska H J 1983 *Solid State Commun.* **48** 293
[5] Pires A S T 1989 *Phys. Rev.* B **40** 9274
[6] Wysin G M, Bishop A R and Oitmaa J 1986 *J. Phys. C: Solid State Phys.* **19** 221
[7] Lemmens L F, Kimura I and Jonge W J M 1986 *J. Phys. C: Solid State Phys.* **19** 139
[8] Borsa F, D'Ariano G and Sona P 1986 *J. Magn. Magn. Mater.* **54–57** 827
[9] Jensen H J, Mouritsen O G, Fogedby H C, Hedegrad P and Svane A 1986 *J. Magn. Magn. Mater.* **54–57** 829
[10] Daniel M, Kruskal M D, Lakshmanan M and Nakamura K 1992 *J. Math. Phys.* **33** 771
[11] Nakamura K, Nakahara Y and Bishop A R 1985 *Phys. Rev. Lett.* **54** 861
[12] Schwinger J 1965 *Quantum Theory of Angular Momentum* ed L C Biedenharn and H van Dam (New York: Academic)
[13] Radcliffe J M 1971 *J. Phys. A: Math. Gen.* **4** 313
Zhang Wei-min, Feng Da Hsuan and Gilmore R 1990 *Rev. Mod. Phys.* **62** 867